

A Comparison of the Noah and OSU Land Surface Models in the ECPC Seasonal Forecast Model

LAUREL L. DE HAAN AND MASAO KANAMITSU

Scripps Institution of Oceanography, University of California, San Diego, La Jolla, California

CHENG-HSUAN LU

NOAA/NWS/NCEP Environmental Modeling Center, Camp Springs, Maryland

JOHN O. ROADS

Scripps Institution of Oceanography, University of California, San Diego, La Jolla, California

(Manuscript received 12 October 2006, in final form 23 March 2007)

ABSTRACT

The Noah land surface model (LSM) has recently been implemented into the Experimental Climate Prediction Center's (ECPC's) global Seasonal Forecast Model (SFM). Its performance is compared to the older ECPC SFM with the Oregon State University (OSU) LSM using two sets of 10-member 50-yr Atmospheric Model Intercomparison Project (AMIP) runs. The climatological biases of several fields tend to increase with the Noah LSM. The differences in near-surface temperature bias are traced to changes in the energy budget. In addition to climatology, the variability and skill (anomaly correlation with observations) of the two ensembles are considered. Unlike the climatology, the near-surface temperature *skill* of the ECPC SFM generally improves with the Noah LSM. Other climatological fields, such as precipitation, show little change in skill.

While the global results are mixed, there are however significant regional improvements over Africa both in terms of climatological bias and skill. In the central African Congo River basin, the Noah LSM removed a warm-dry bias and improved upon the near-surface temperature skill of the OSU LSM. In the African Sahel, the Noah LSM greatly enhanced the climatology, variability, and skill of the ECPC SFM as well as improving the location of the African easterly jet.

1. Introduction

A major objective of the Global Energy and Water Experiment (GEWEX) has been to develop land surface models (LSMs) for research, application, and prediction. LSMs developed for these purposes have included the Variable Infiltration Capacity model (VIC; Liang et al. 1994; Peters-Lidard 1997), the National Center for Atmospheric Research's (NCAR's) Common Land Model (CLM; Bonan et al. 2002), the National Aeronautic and Space Administration's (NASA's) Mosaic (Koster and Suarez 1992), and the land surface

model Noah (Ek et al. 2003). Noah was developed jointly by the National Centers for Environmental Prediction (NCEP), Oregon State University (OSU), the Air Force, and the Hydrology Research Laboratory at the National Weather Service under the sponsorship of the National Oceanic and Atmospheric Administration (NOAA) Office of Global Programs (OGP) and was implemented in NCEP's regional Eta model and its data assimilation system (EDAS) in the mid-1990s. Noah was recently implemented into NCEP's Global Forecast System (GFS) and Global Data Assimilation System (GDAS) in 2005.

The performances of the Noah LSM over the continental United States, both in an uncoupled land data assimilation [the North American Land Data Assimilation System (NLDAS); Mitchell et al. 2004a] and in coupled numerical model assimilations [the Eta-EDAS suite and North American Regional Reanalysis (NARR);

Corresponding author address: Laurel DeHaan, Climate Research Division, Scripps Institution of Oceanography, University of California, San Diego, Mail Code 0224, 9500 Gilman Dr., La Jolla, CA 92093-0224.

E-mail: ldehaan@ucsd.edu

Mitchell et al. 2004b, Mesinger et al. 2006] have been studied extensively. The NLDAS compared the strengths and weaknesses of the previously mentioned LSMs for variables directly linked to the LSMs (such as runoff, soil moisture, and snow cover) when all were forced by the same observed precipitation, downward solar and terrestrial radiation, and near-surface meteorology. The results, while not intended for rating the LSMs, did show that the Noah LSM is of the same caliber as the other state-of-the-art LSMs, at least over North America. The global performance of the LSMs was studied in the Global Soil Wetness Project (GSWP; Dirmeyer et al. 2006) and the Global Land Data Assimilation System (GLDAS; Rodell et al. 2004). Again in these studies, the Noah LSM continues to be part of the evolving suite of preferred global as well as regional LSMs.

In addition to looking at the performance of the LSMs, many people have also studied the impact of land surface processes in coupled land-atmosphere general circulation models (GCMs). Garratt (1993) provides a review of studies on the sensitivity of GCMs to land surface processes from the late 1970s to the early 1990s. Since then there have been many other global studies including: Delage and Versegny (1995), Roads et al. (1999), Koster et al. (2002), Maynard and Polcher (2003), Lu et al. (2005), Dirmeyer (2005), and DeHaan and Kanamitsu (2007) to name but a few. These studies considered the impact of the land surface processes on a number of global fields including sensible heat flux, precipitation, variability, and predictability. Suffice it to say that it is important that a LSM perform well both regionally and globally. Historically, however, some unconstrained LSMs have had a noticeable deleterious effect on the climate (e.g., Roads et al. 2003).

In this study we are concerned with whether an unconstrained coupled model, the Experimental Climate Prediction Center's (ECPC's) global Seasonal Forecast Model (SFM), using the Noah LSM could improve the climatology and variability over the OSU LSM (Pan and Mahrt 1987), which is the predecessor to the Noah scheme, and then whether the Noah LSM could enhance the skill of global temperature and precipitation (and perhaps other variables). Currently the operational NCEP Climate Forecast System (CFS; Saha et al. 2006), which makes multiseason forecasts each month, still uses the OSU LSM. By contrast, the current operational NCEP GFS, which makes medium-range forecasts every day, uses the Noah LSM. Given the presumable overall improvements by the Noah LSM over North America, the next implementation of the

CFS will incorporate the Noah LSM. The anticipation of this change further motivated our study.

Section 2 provides a brief summary of the differences between the OSU and Noah formulation. Section 3 provides a brief overview of the ECPC SFM, which is very similar to the NCEP reanalysis-1, reanalysis-2, CFS, and GFS family of models. In fact, the predecessor to the ECPC SFM was the NCEP SFM, which was replaced in 2005 with the CFS. Sections 4, 5, 6, and 7 examine the climatology, energy balance, variability, and skill (anomaly correlation with observations). Section 8 looks at the soil moisture lag correlations. Section 9 shows in more detail the clear improvements over Africa. Section 10 attempts to attribute changes in the simulations to changes in the LSM physics. Section 11 provides our conclusions. We were somewhat disappointed that, with the exception of Africa, the skill increases were modest. In that regard, it should be noted that we were using Noah 2.6 and some skill enhancements may be possible with Noah 2.7; however, an assessment of this will require another set of global ensemble experiments.

2. Comparison of OSU and Noah formulations

a. OSU scheme

The original OSU land model was developed in the 1980s (Mahrt and Ek 1984; Mahrt and Pan 1984; Pan and Mahrt 1987; Ek and Mahrt 1991). It is a multilayer soil model, which uses the Penman potential evaporation approach and applies an extension of the simple canopy resistance formulation. The land model used in this study has two soil layers: 10 and 190 cm thick. The soil moisture and ground temperature in these two layers are predicted. In addition, the water content of the canopy and the water equivalent snow amount are also predicted.

The evaporation at the surface has three components: direct evaporation from the top 10 cm of bare soil, transpiration from vegetation, and evaporation from the canopy partitioned by the vegetation cover that varies geographically as well as seasonally. The surface skin temperature is the diagnostic quantity from the surface energy balance.

The soil temperatures are predicted using the diffusion equation. The top boundary condition is the skin temperature and the bottom boundary condition is an annually averaged climatological deep soil temperature. The thermal diffusivity is dependent on the soil type and its water content.

The hydrology of the soil layer is determined by Richardson's equation, which consists of diffusion, gravitational percolation, transpiration, precipitation

(excluding the part retained by the canopy), surface runoff, and base flow runoff. The transpiration is partitioned according to the thickness of the soil layer and is proportional to the vegetation fraction, potential evaporation, and a factor that depends on canopy resistance including soil moisture stress (Ek and Mahrt 1991). The transpiration also depends on the canopy water content. The potential evaporation is obtained following Mahrt and Ek (1984). The direct evaporation from soil is formulated by Chen and Dudhia (2001) and Mahfouf and Noilhan (1991), which showed an advantage over the original Mahrt and Pan (1984) formulation in short-range prediction and in regional downscaling experiments (Betts et al. 1997; Kanamitsu and Mo 2003). The direct evaporation is proportional to the potential evaporation and the ratio of the excess of soil moisture over the wilting point to the excess of field capacity over the wilting point. Additional details about the slightly updated OSU scheme can be found in Chen et al. (1996).

b. Noah scheme

The Noah land model is an improved version of the OSU scheme described above, but with several significant changes (Koren et al. 1999; Ek et al. 2003). First, the number of soil layers is increased from two (10 and 190 cm thick) to four (10, 30, 60, and 100 cm thick) and the root zone depth is spatially varying (dependent on vegetation classes) rather than fixed (2 m for all vegetation classes) as in the OSU. Furthermore, the volumetric soil ice content at each soil layer is added as a new prognostic variable. The ice content is predicted as a function of soil temperature, soil moisture content, and soil type. The ice content in the soil water significantly influences the infiltration rate. Note that total and liquid soil moisture are prognostic state variables and the difference between the two represents frozen soil moisture. The frozen soil physics (Koren et al. 1999) includes the impact of soil freezing/thawing on soil heat sources/sinks, vertical movement of soil moisture, soil thermal conductivity and heat capacity, and surface infiltration of precipitation. Snowpack physics are also improved with the snow density predicted as a function of time and snow temperature. The snow thermal conductivity is affected by the change in snow density and thus the snowmelt process is more accurately simulated. The snow albedo is also predicted considering the partial snow cover in the grid box, which is a function of snow depth. The deep-snow albedo is constrained by the geographically varying annual maximum snow albedo dataset as a function of vegetation type. To summarize, the prognostic variables of the Noah scheme used in this study are soil temperature,

moisture and soil ice content at four soil layers, canopy water content, snow depth, snow density, and snow albedo.

Bare soil evaporation by Mahrt and Pan (1984) used in the original OSU scheme is replaced with a new formulation, which is more similar to the OSU model utilized in the first ECPC SFM with further modification by a second-power dependency on the soil moisture saturation ratio. There are also several small refinements to the formulation of ground heat flux, canopy conductance, surface runoff and infiltration, soil thermal conductivity, and its dependence on vegetation and transpiration.

c. Noah's performance for the continental United States

In an earlier paper on the Noah LSM, Ek et al. (2003) found the changes in snowpack and the addition of frozen soil physics reduced the cold wintertime bias of a mesoscale model, while the bare soil evaporation and soil thermal conductivity reduced a springtime warm bias. Several other papers have looked at the qualities of the Noah LSM in the context of the NLDAS. The NLDAS used four state-of-the-art LSMs in an offline mode with a fine grid for 3 yr to study the differences between the models. A summary of the nine papers resulting from this project can be found in Mitchell et al. (2004a). Following are some of the results specific to the Noah LSM. Schaake et al. (2004) and Robock et al. (2003) found that both the range and magnitude of soil moisture by the various models agreed with observations in select locations. However, the Noah LSM underestimated the snow water equivalent (Pan et al. 2003) and underestimated the snow cover extent, partially due to the low snow albedo (Sheffield et al. 2003). The land surface temperature had a high bias in many areas in the Noah LSM, even though it estimated surface energy fluxes well (Mitchell et al. 2004a; Robock et al. 2003). Both Robock et al. (2003) and Mitchell et al. (2004a) concluded that the aerodynamic conductance was too low in the Noah LSM and that the canopy resistance was too high. Overall, however, the Noah LSM proved to be a viable land surface model.

3. General circulation model and experiment

The ECPC SFM is used for this study (Kanamitsu et al. 2002a). It has a horizontal resolution corresponding to T62 (192×94 global grid) with 28 vertical levels. The model has relaxed Arakawa–Schubert convection (Moorthi and Suarez 1992), Chou's shortwave and longwave radiation (Chou and Suarez 1994; Chou and Lee 1996), Slingo's (1987) cloud scheme, Tiedtke's

TABLE 1. ECPC and NCEP global model characteristics. The abbreviation “dep.” stands for “dependent”; “mon.” stands for “monthly.”

	ECPC SFM	NCEP GFS	NCEP CFS	R2	RI
Resolution	T62rL28	T384L64	T62L64	T62L28	T62L28
Convection	RAS ^a	SAS ^b	SAS ^b	SAS ^b	SAS ^b
SW radiation	M. D. Chou ^c	Modified M. D. Chou ^d	Modified M. D. Chou ^d	M. D. Chou ^c	Lacis and Hansen ^b
LW radiation	M. D. Chou ^c	AER RRTM ^f	AER GFDL ^f	Fels and Schwarzkopf ^b	Fels and Schwarzkopf ^b
Clouds	Slingo ^g	Zhao and Carr ^a	Zhao and Carr ^a	Lookup table ^b	Lookup table ^b
PBL	Nonlocal ^c	Nonlocal ^c	Nonlocal ^c	Nonlocal ^c	local, RI dep. ^b
Gravity wave	Alpert et al. ^b	Kim and Arakawa ^h	Kim and Arakawa ^h	Alpert et al. ^b	Alpert et al. ^b
Land surface	OSU two-layer, ^b Noah 2.6 ⁱ	Noah 2.7 ⁱ	OSU two-layer ^b	OSU two-layer obs P drives soil moisture ^c	OSU two-layer soil moisture correction ^b
Vegetation	USGS mon. ^j	USGS mon. ^j	USGS mon. ^j	Fixed vegetation cover ^b	Fixed vegetation cover ^b
Soil type	USGS ⁱ	USGS10 ^c	USGS ⁱ	Fixed ^b	Fixed ^b
Orography	Smooth ^c	Mean	Mean	Smooth ^c	Enhanced ^b
Ozone	Climatology ^b	Predicted from analysis ^b	Predicted ^b	Climatology ^b	Climatology ^b
SST	2-tier coupled	Obs fixed	1-tier coupled	Obs	Obs
Sea ice	Climatology ^b	Sea ice model ^k	Climatology ^b	Analysis ^b	Analysis ^b

^a Zhao and Carr (1997).

^b Differenced in Kalnay et al. (1996).

^c Differenced in Kanamitsu et al. (2002a).

^d Hou et al. (2002).

^e Chou and Suarez (1994).

^f Mlawer et al. (1997).

^g Slingo (1987).

^h Kim and Arakawa (1995).

ⁱ Ek et al. (2003).

^j Kanamitsu and Mo (2003).

^k Winton (2000).

(1983) shallow convection, large-scale condensation, gravity wave drag (Alpert et al. 1988), and smoothed mean orography. This model has been used since 2002 to produce a seasonal forecast every month at ECPC, which is provided to the International Research Institute (IRI) multimodel forecast, as well as to the Climate Prediction Center at NCEP and other forecasters. There was increased enthusiasm about the forecasts after adding the Noah LSM, especially about the African forecasts, and consequently the forecasts currently provided all use the Noah LSM.

Table 1 summarizes the similarities and differences of the ECPC SFM with the NCEP GFS, CFS, and both reanalysis-1 (R1; Kalnay et al. 1996) and reanalysis-2 (R2; Kanamitsu et al. 2002b). There are several differences with key physical processes between the models. Particularly noteworthy are the differences in convective parameterization, radiation and cloudiness, and the ocean component of the coupled system (Yulaeva et al. 2007). These differences make it somewhat difficult to directly apply the results obtained in this study to NCEP operational models or to other models. The general applicability of this result can be strictly verified by

applying the same LSM to different models and performing similar long ensemble integrations.

To look at the effects of the LSMs on the skill of the simulation, two sets of ensembles were integrated with the ECPC SFM: one with the OSU LSM and the other with the Noah LSM. These ensemble integrations will be referred to simply as Noah and OSU. Both ensembles were run continuously for the years 1950–2001. Both ensembles had 10 members, where each member was initialized with slightly different atmospheric initial conditions. The initial conditions for both the land and atmosphere came from reanalysis data (R1), with the 10 members coming from 10 consecutive days. Both ensembles were also forced with the same observed sea surface temperatures (SSTs). The methodology is perhaps quite strict (500+ years for each model configuration). However, these large historical ensembles make it possible to calculate statistically significant estimates of the actual skill of the model, given that the change in skill due to land surface parameterization is known to be small.

The observed SSTs were taken from the 40-yr European Centre for Medium-Range Weather Forecasts

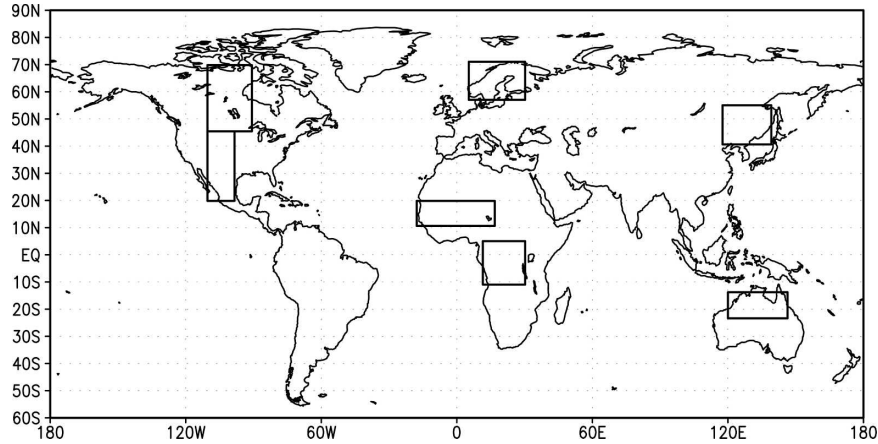


FIG. 1. Map of the regions considered in detail: central Canada, the south-central United States, Scandinavia, the Sahel, the Congo River basin, northern China, and northern Australia.

(ECMWF) Re-Analysis (ERA-40) dataset, based on the Hadley Centre Sea Surface Temperature dataset (HadSST) and the Extended Reconstructed Sea Surface Temperature (ERSST) but updated by the ECMWF for their use in ERA-40. The observations (truth) for the evaluation of most climatological values of the simulation are taken from the NCEP Department of Energy (DOE) reanalysis or R2. The accuracy of the climatologies of the reanalysis data for temperature, geopotential heights, and winds are comparable to that of other available analyses (Basist and Chelliah 1997). As shown in Table 1, the reanalysis (R2) uses the OSU LSM and nudges the soil moisture based on observed precipitation (Lu et al. 2005). The monthly mean soil moisture in R2 has reasonable temporal correlations to observations (Lu et al. 2005). The observations used for the precipitation climatology come from the Climate Prediction Center Merged Analysis of Precipitation (CMAP), since it is considered more accurate than the reanalysis. For computing the skill of temperature and precipitation, a longer data assimilation is preferred, so the observed record is from the Climate Research Unit (CRU) at the University of East Anglia, Norwich, United Kingdom (hereafter called CRU data).

Throughout this study we will focus on several regions of interest, which are shown in Fig. 1, in addition to a global overview. The African Sahel (10°–20°N, 345°W–15°E) and the Congo River basin of central Africa (10°S–5°N, 12°–30°E) are of interest due to large improvements with Noah. The south-central United States (20°–45°N, 110°–98°W) was chosen because it has often been shown to have sensitivity to land surface processes (i.e., Koster et al. 2004). Scandinavia (56°–75°N, 5°–30°E) gives an example of the northern lati-

tudes, while northern Australia (22°–13°S, 120°–145°E) gives an example of the Southern Hemisphere. Central Canada (45°–70°N, 110°–90°W) is considered because of a large warm bias there. Finally, an area of northern China and eastern Russia (42°–55°N, 115°–140°E) shows the largest loss of skill with Noah.

All the skill comparisons are based on the temporal correlation between the ensemble simulations and CRU observations at each grid point. This measure is probably most useful for climate prediction, since our main interest is whether it is going to be warmer/colder/drier/wetter than usual. We should note that we intentionally avoided removing long-term trends in our calculation. Thus, the skill measure in this paper represents skill of the model on all time scales. We will see the implication of this definition of skill in section 9.

4. Climatologies

A basic element of the differences between the integrations using the Noah and OSU LSMs is the model climatology based on the ensemble average. In this section we present several climatologies. Significance tests have been performed on all the differences shown and it was found that, except in cases of very small differences, the results shown are significant at the 99% level based on a *t* test. For example, all differences greater than 0.1° are significant for 2-m temperature. The statistical significance of the differences is not surprising given the reasonably large sample size of this study.

It is evident from the difference in 2-m temperature climatology (the first column of Fig. 2) that Noah often produces a significantly warmer climatology than OSU in the northern latitudes. The difference in temperature occurs through much of Asia, Europe, and North America for all four seasons. Presumably, in the cold

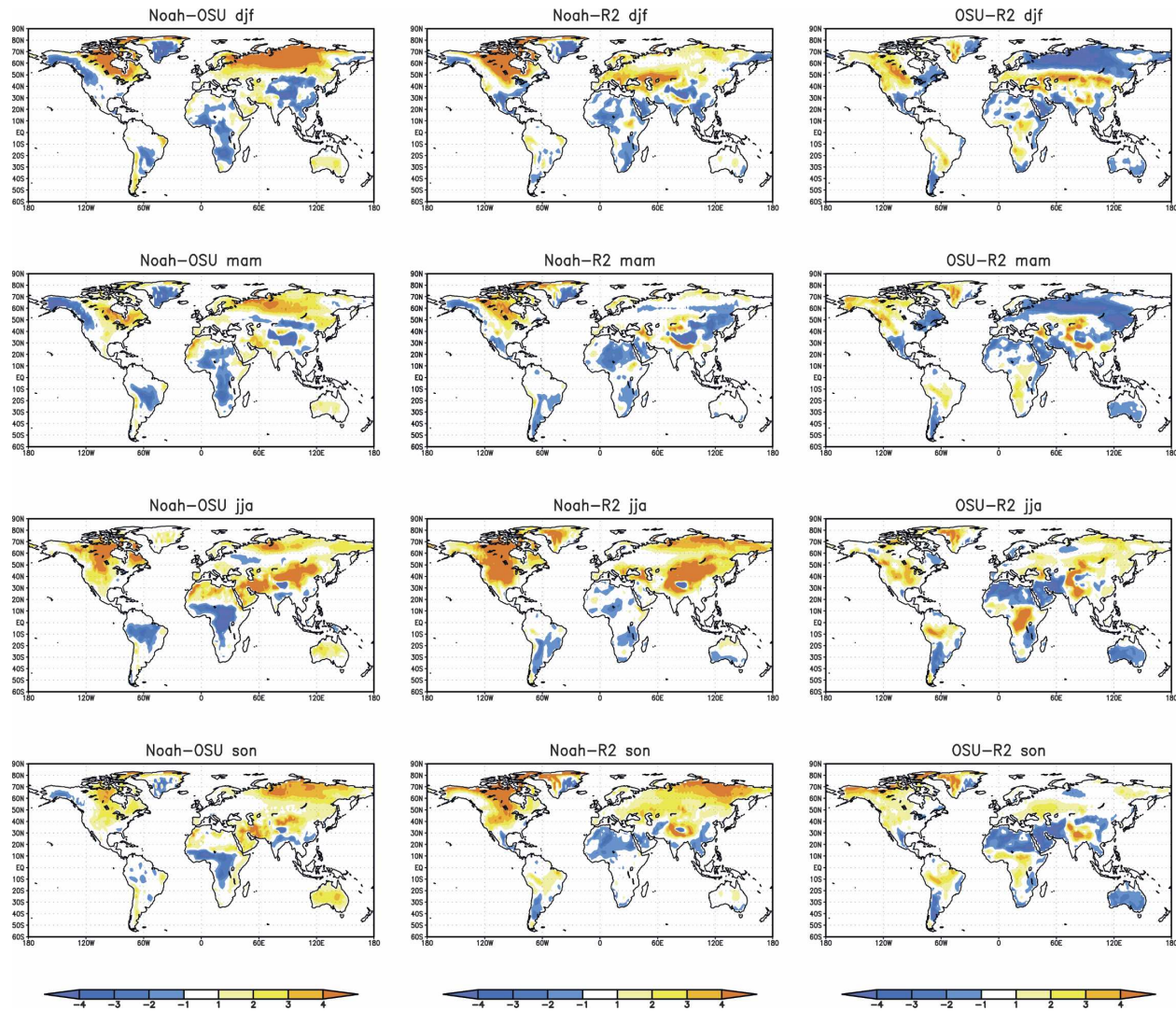


FIG. 2. Near-surface temperature climatological differences between (middle) Noah and (right) OSU and R2, and (left) between Noah and OSU (top to bottom) for all four seasons (in K).

seasons, this difference is due in part to the changes in handling of ice and snow, while in the warm seasons it could be related to the canopy resistance, as discussed in Mitchell (2004a). There are also a few areas where Noah is colder than OSU, primarily Alaska in March–May (MAM), the Himalayas in December–February (DJF) and MAM, and year-round in Africa.

Comparing the model 2-m temperature climatologies to the NCEP–NCAR reanalysis-2 data (Fig. 2, columns 2 and 3) it can be seen that Noah has a warm bias in some areas in some seasons, particularly over Russia, western China, and North America in June–August (JJA) and September–November (SON), and in central Canada throughout the year. A comparison of CRU observations and Noah (not shown) produces a similar

pattern, with large warm biases in the northern latitudes and smaller cold biases in the Tropics. In contrast, OSU has a strong cold bias over most of Russia in DJF and MAM. The warm bias in North America is also noticeable, but is smaller than that of Noah.

While some Noah biases are large, there are areas where the Noah climatology is closer to the reanalysis and CRU data than OSU. Those areas include northern Eurasia in DJF and MAM (where OSU has a large cold bias), central Africa in JJA (around the Congo River basin), and Australia almost year-round. In general Noah produces larger temperature biases than OSU in the northern latitudes in JJA and SON. In the Tropics the magnitude of the biases are similar between the two LSMs.

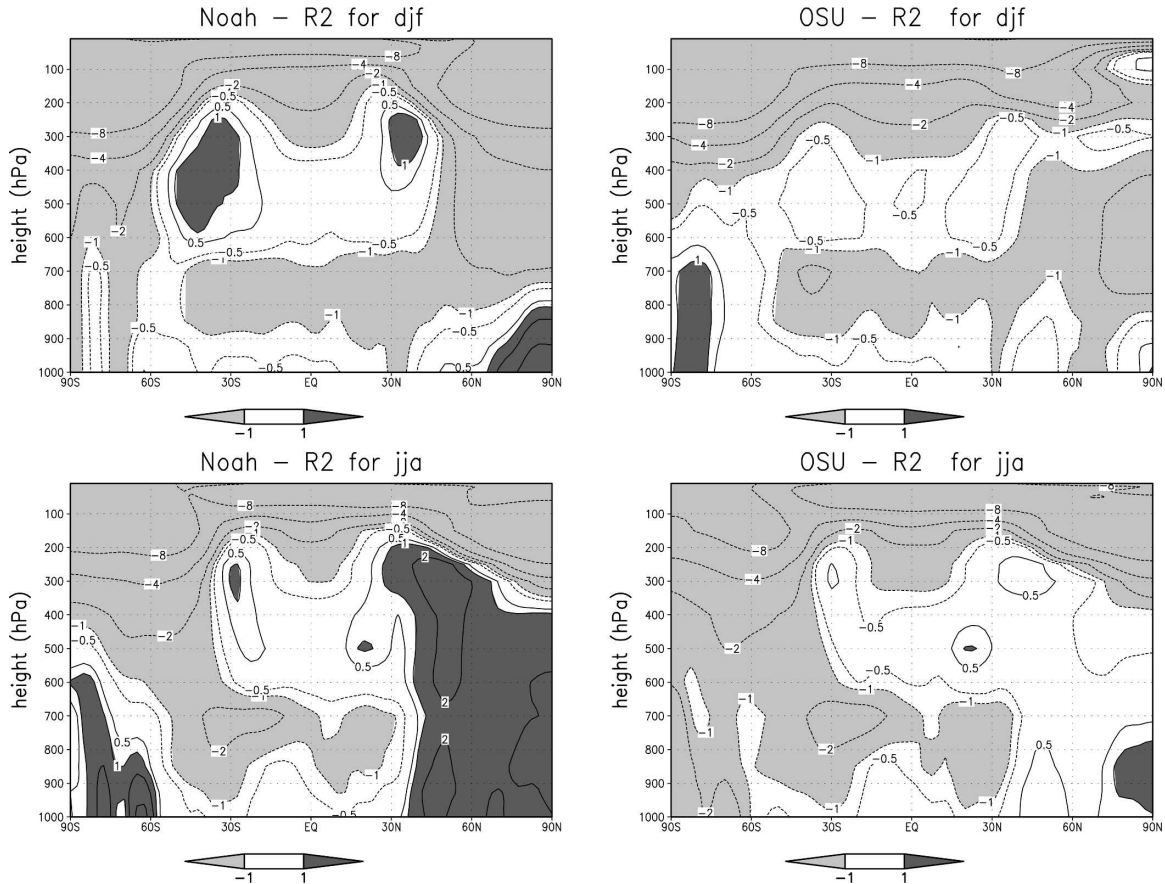


FIG. 3. Zonal mean of climatological temperature differences (in K) between (left) Noah and R2 and (right) OSU and R2 for (top) DJF and (bottom) JJA.

In the zonal cross section of temperature (Fig. 3) the average bias is somewhat greater for Noah than for OSU. In the subtropical upper troposphere in DJF, Noah is significantly warmer than OSU due to the increase in precipitation to be discussed later. The high-latitude warm bias with Noah extends to about 200 hPa in JJA, however in DJF it is limited to the lower levels.

The largest difference in 500-hPa height between the two ensembles is in the arctic in DJF (Fig. 4). Farther south, a height increase with Noah in the midlatitude Pacific leads to the weakening and northward shift of the climatological trough. In the Southern Hemisphere in DJF, a band of positive bias appears at about 40°–50°S in Noah, shifting the Southern Hemisphere subtropical jet farther south.

Looking at the difference in the precipitation rate (Fig. 5), large differences appear over the Southern Hemisphere land during DJF, while the differences are more confined to the Tropics in JJA. It can be seen that Noah generally has more rainfall over land, and OSU has more rainfall over the oceans, indicating an apparent impact of the land scheme and global adjustments

of precipitation in the model. While the climatological precipitation from Noah and OSU are closer to each other than they are to CMAP observed precipitation, there are some notable differences. The annually averaged precipitation rate from OSU *over land* between 30°S and 30°N is higher than observed; however, Noah has an even higher precipitation rate, approximately 30% more than OSU. This larger precipitation rate could be related to the increase in temperature over the tropical upper troposphere mentioned earlier, with the enhanced moist convection releasing more latent heat. Over the oceans Noah is slightly closer to observations than OSU with a 5% reduction in the precipitation rate with Noah. Again, the global bias with Noah is somewhat larger than that with OSU.

A noteworthy difference in precipitation is over tropical Asia (Indochina and Indonesia), where Noah is drier over southern India, Thailand, and the northern Philippines and wetter to the north and south during JJA. Both models are wetter than CMAP observations in this region, but the maximum rainfall is shifted northward in Noah. This makes the southern portion closer

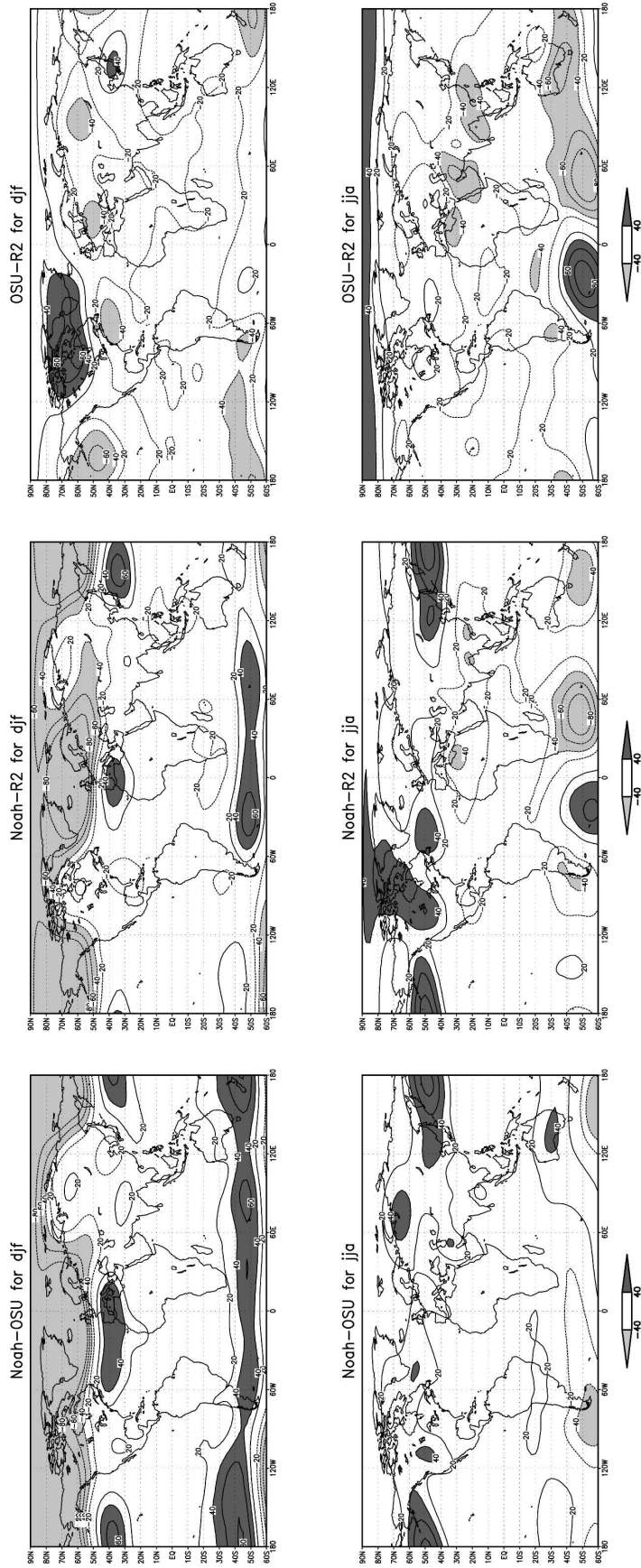


FIG. 4. Climatological 500-hPa height differences between (left) Noah and OSU, (middle) Noah and R2, and (right) OSU and R2 for (top) DJF and (bottom) JJA (in m).

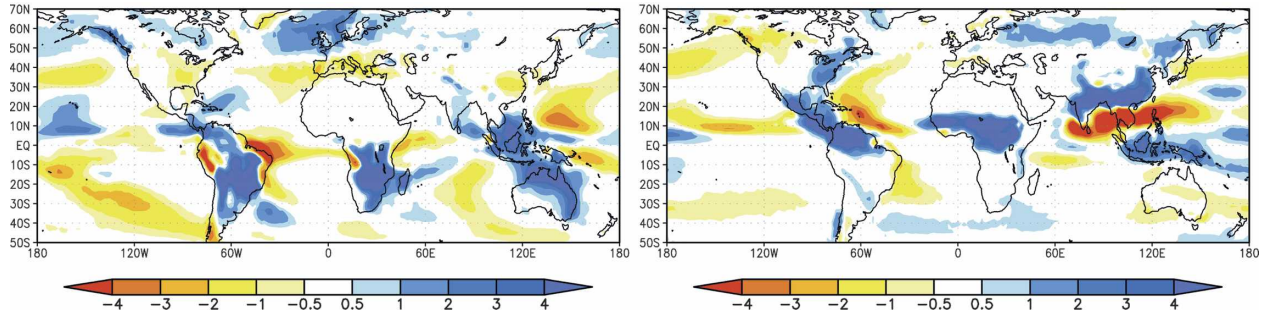


FIG. 5. The difference between Noah and OSU climatological precipitation for (left) DJF and (right) JJA (in mm day^{-1}).

to observations than OSU but the northern portion farther from observed values.

Another interesting difference is the intertropical convergence zone (ITCZ) over Africa in JJA, where Noah has a more accurate precipitation rate (Fig. 6). Here the average precipitation from Noah is within 20% of CMAP, while OSU produces less than half of the rainfall of CMAP. Noah also reproduces the location of rainfall more accurately than OSU reaching farther north than OSU, which is significant for the Sahel region. Noah does, however, have too much precipitation east of about 15°E .

Looking at soil moisture, we find that OSU tends to be dryer than reanalysis-2, while Noah is usually wetter than reanalysis-2 (Fig. 7). This is not surprising based on the difference in precipitation. The root zone of OSU, which always extends to 2 m, could also add to the dryness of OSU. Typical differences in volumetric soil moisture between the two LSMs can be seen in the south-central United States and northern China. The largest differences in soil moisture between the two ensembles are in Africa. In both central Africa and the Sahel, Noah is quite close to the reanalysis and OSU is very dry. The central African region is the same region where Noah had an improved temperature climatology over OSU, showing that Noah removes a warm-dry bias of OSU.

These comparisons of the climatologies of various parameters between Noah and OSU indicate that the land model is responsible for some of the biases appearing in the simulations, particularly the temperature bias in the northern regions and the precipitation bias over land. Further improvements (and tuning) of the frozen soil model and vegetation characteristics seem to be necessary to reduce these biases. The land model also influences the geographical distribution of precipitation including the distribution of precipitation between the land and ocean. The land model is responsible for the warm bias in the tropical upper troposphere through changes in precipitation. In the Tropics, the model skill seems to be affected by the bias, as shown later.

5. Energy balance

Given the difference in temperature between Noah and OSU, it is worthwhile to look at the differences in the energy budgets of the two ensemble simulations to identify the sources of the differences. We will focus on the JJA budget for central Africa (where OSU has a warm bias), the south-central United States (where Noah has a warm bias) and central Canada (where the Noah warm bias persists throughout the year). Figure 8 shows the difference of surface fluxes between OSU

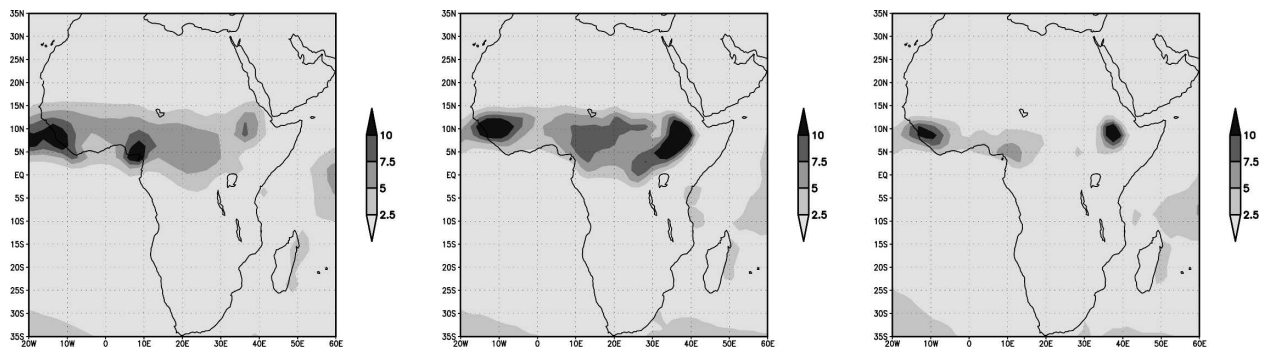


FIG. 6. Climatological precipitation for JJA from (left) CMAP, and the ensembles (middle) Noah and (right) OSU (in mm day^{-1}).

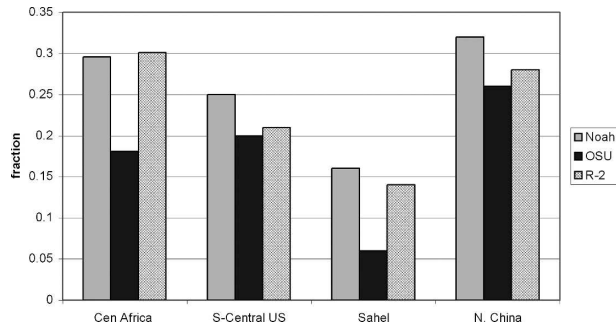


FIG. 7. Vertically integrated, annually averaged, volumetric soil moisture for central Africa, the south-central United States, the Sahel, and northern China for Noah, OSU, and R2.

and Noah (Noah minus OSU) as well as albedo, total cloud cover, and near-surface temperature. A positive value always indicates that Noah has the larger value, regardless of the direction of the flux. The differences shown are all statistically significant at the 99% level based on a t test, with the exception of extremely small differences and shortwave downward radiation for the United States.

The top panel in Fig. 8 (central Africa) shows that the lower temperature in Noah is largely due to an increased latent heat flux with an additional contribution of less downward shortwave flux at the surface. The decrease in upward shortwave flux at the surface, which is consistent with the decrease in albedo, is compensated by the decrease in downward shortwave flux. This difference in the energy budget suggests that the wetter soil in Noah is responsible for more evaporation, less shortwave radiation reaching the ground, and lower temperatures over central Africa. The decrease in longwave radiation is dependent on the vertical distribution of moisture, temperature, and clouds, and is difficult to explain. The increase in cloudiness is also consistent with more moist air over the area.

Over central Canada, the considerable warm bias in Noah is consistent with the increase in sensible heat flux from the surface. This increase is caused by an increase in downward shortwave and longwave radiation fluxes. The decrease in albedo also contributes to more absorption of the shortwave flux at the surface, causing warming. A very large decrease in ground flux, which also contributes to the warming, is noted, but this seems to be due to an abnormally large downward ground heat flux in OSU. The Noah cloudiness is less for high and low clouds, which is very likely the source of the increased downward radiation flux reaching the surface and causing the warm bias.

Over the central United States, the differences in surface fluxes are very similar to those over central

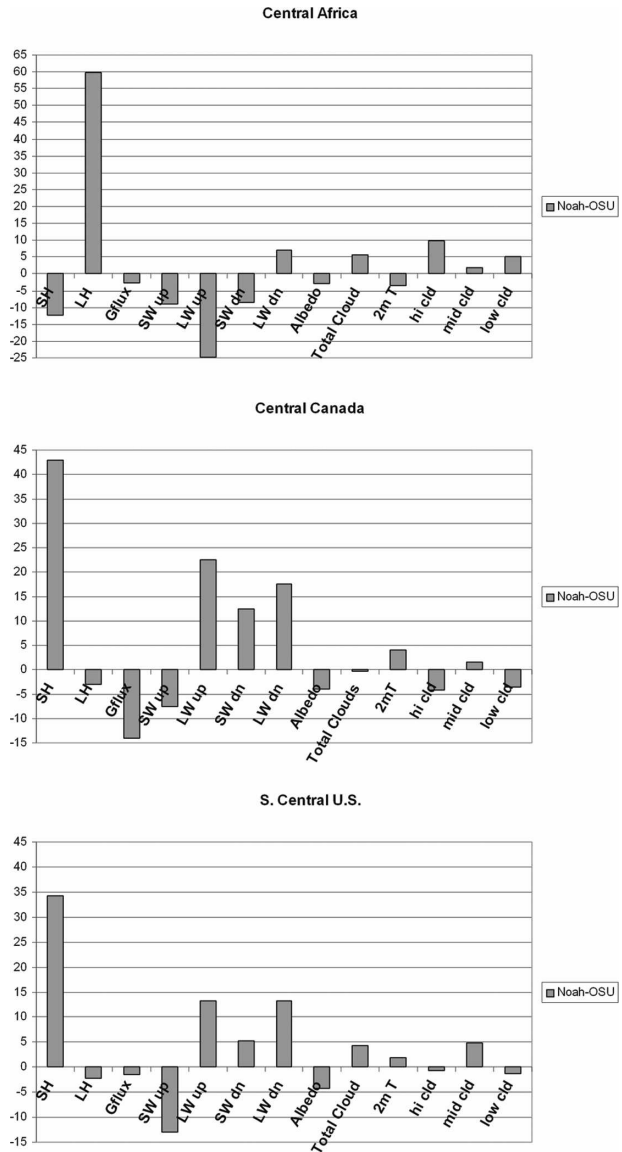


FIG. 8. Energy balance difference between Noah and OSU in JJA for (top) central Africa, (middle) central Canada, and (bottom) the south-central United States. Sensible heat (SH), latent heat (LH), ground flux (Gflux), shortwave upward radiation (SW up), longwave upward radiation (LW up), shortwave downward radiation (SW dn), and longwave downward radiation (LW dn) are in units of $W m^{-2}$. Albedo, total, high, middle, and low cloud are percents. The 2-m temperature (2m T) is in units of kelvin.

Canada. The smaller difference in the ground fluxes and high and low cloudiness in the central United States is noteworthy. The change in the midlevel cloud may not be consistent with the increase in downward radiation fluxes (which also shows up over central Canada, although its magnitude is much smaller). For both central Canada and the central United States, it

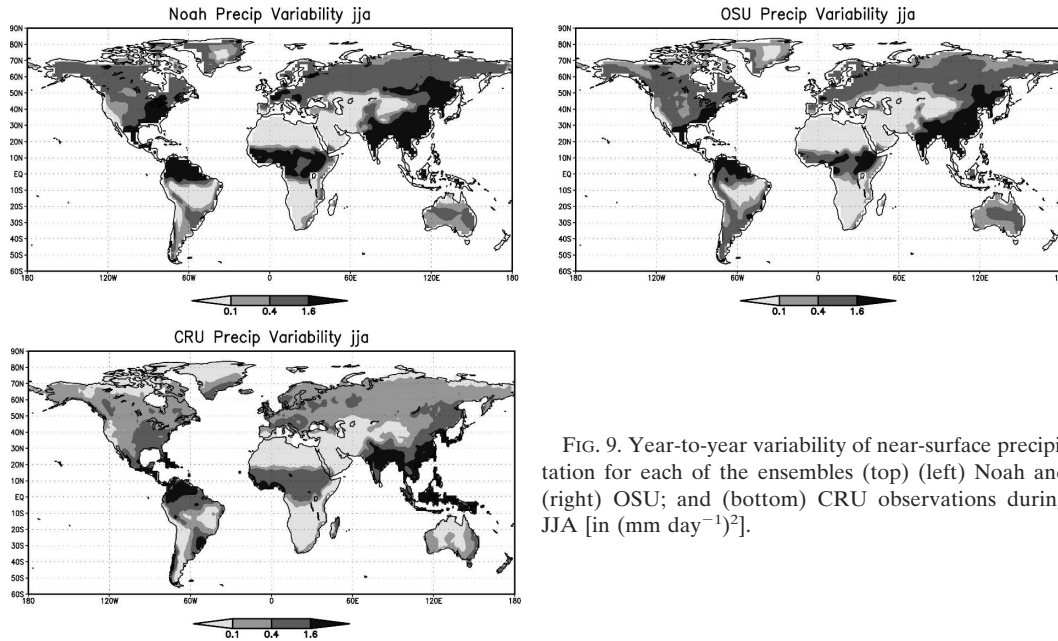


FIG. 9. Year-to-year variability of near-surface precipitation for each of the ensembles (top) (left) Noah and (right) OSU; and (bottom) CRU observations during JJA [in $(\text{mm day}^{-1})^2$].

seems that a sizable contribution of warming over these areas is the change in large-scale features, which causes the difference in the atmospheric temperature and moisture. Specifically, stronger ridging over North America in the Noah climatology, seen in Fig. 4, may be the reason for higher incident shortwave fluxes and consequently higher surface temperatures. It is also worth mentioning that there is a positive feedback between the temperature and energy budget, as higher temperatures encourage ridging.

6. Variability

Figure 9 shows the year-to-year variability of the seasonal mean precipitation in JJA, computed as the variance from individual ensemble members. In most areas of the globe there is not a statistically significant difference in the variability of 2-m temperature between the two LSMs, so that result is not shown. Looking at precipitation the models also have similar variability, but the differences are usually significant. Noah has about 15% more variability than the OSU ensemble globally averaged, but twice the variability of observations. A close look at Africa shows that while Noah generally has too much variability, the band of maximum variability is shifted about 4° to the south with OSU. Both observations and Noah have relatively large variability to approximately 18°N , while OSU only has large variability to approximately 14°N . As with the precipitation climatology, this shifting is significant for the Sahel region.

The model's larger variability compared to observations certainly points to a problem in both land schemes, as well as to the precipitation processes in the model. The tendency of the models to have too many extremes is a well-known model problem, but is not well understood.

7. Skill

Considering the globally averaged 2-m temperature skill seen in the top panel of Fig. 10, we see the similarity in skill between the two ensembles. (Skill is defined as the temporal correlation of seasonal means with CRU data.) However, Noah does perform better than OSU in the summer and fall, while OSU does better than Noah in the spring. These differences are significant at the 95% confidence level. The difference in DJF shown here is not statistically significant.

A simple difference, however, between the skills of the two ensembles is not always a good comparison. In some cases, even though one LSM produces higher skill than the other, neither has useful skill. To look at this more clearly we will only consider the areas where the skill is at least 0.3, which is considered to be at least marginally useful for forecasters. The light gray columns in the bottom panel of Fig. 10 show the globally averaged difference in skill between the two LSMs in areas where Noah has skill of at least 0.3, while the dark gray columns show the difference in skill where OSU has skill of at least 0.3. This figure shows, in SON for example, that in the areas where Noah performs well, the

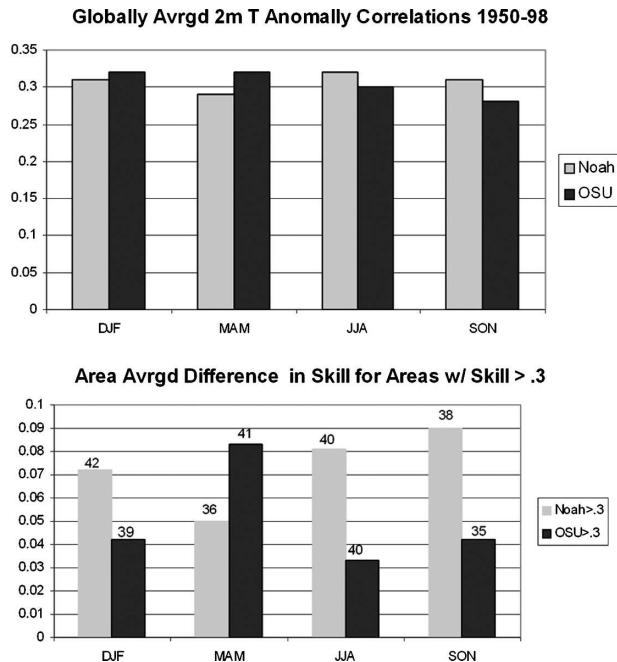


FIG. 10. Correlations between modeled 2-m seasonal mean temperatures and CRU observations averaged over the global domain. (top) The correlation averaged over all land areas for both Noah and OSU. (bottom) The difference in correlations between Noah and OSU averaged only over areas with a correlation greater than 0.3; the numbers on top of the columns represent the percentage of land area where the correlations exceed 0.3 for the Noah or OSU LSMs, respectively (see text for more details).

increased skill over the OSU ensemble is 0.09, while in areas where OSU performs well, the increased skill over Noah is about 0.04. The numbers on top of the columns show the percentage of land area used in computing the difference, or in other words, the percentage of area with skill greater than 0.3 for that ensemble. We see here that in three of the four seasons Noah improves upon the OSU ensemble in the areas where there is skill. Most notably, there is now a significant increase in skill in DJF with Noah. While the improvements with Noah are clearly modest on a global scale, more often than not Noah does lead to improvements in skill in all seasons except MAM.

Looking regionally, we consider six of the regions mentioned previously (Scandinavia, northern Australia, the south-central United States, northern China, central Africa, and the Sahel), which are shown in Fig. 11. Many of the regions have mixed results, with some seasons having greater skill with Noah and other seasons having greater skill with OSU. Scandinavia (Fig. 11a) is somewhat typical of many northern latitude regions, which do not show any improvement in skill with Noah in DJF, MAM, or JJA, but have a significant improvement in SON. The opposite is true for northern

Australia (the only region completely in the Southern Hemisphere considered here), where Noah improves the skill in DJF, MAM, and JJA, but not SON. This, as with the globally averaged skill, suggests that Noah tends to have the highest skill in the fall and the lowest skill in the spring relative to OSU. In the south-central United States (Fig. 11c) there is only one occurrence of skill greater than 0.3, which is in JJA with Noah. In southeast Russia and northern China (Fig. 11d) there is a loss of skill in DJF and MAM with Noah. This is the largest area of skill loss with Noah. In central Africa, on the other hand, Noah produces a higher skill in all four seasons. Again, this is the region where Noah also had improved temperature and soil moisture climatologies. The African Sahel (Fig. 11f) shows increases in near-surface temperature skill in all seasons also, but most notably in JJA (during the monsoon).

Considering temporal precipitation correlations (not shown), both versions of the model show similar skill, with the vast majority of the skill in the Tropics. Globally averaged, Noah has significantly higher skill than OSU in JJA, but there are no significant differences in the other three seasons.

8. Soil moisture time lag correlations

Since the SSTs are identical in Noah and OSU, it is reasonable that in some cases improved skill could be related to a longer soil moisture memory, which may differ between the ensembles. This requires that the Atmospheric Model Intercomparison Project (AMIP) simulations can produce reasonably accurate soil moisture estimates in some locations, as longer soil moisture memory in regions with poor soil moisture estimates do not improve the skill. Our study, however, did not find any such regions. We have computed the soil moisture time lag correlation out to four months for the areas shown in Fig. 11 (as well as other areas that are not shown). The time lag correlation was computed for each of the three months in a given season and then averaged.

In general there was not a clear relationship between the soil moisture time lag correlations and the skill (Fig. 12). For example, in Scandinavia in SON, when Noah has higher skill, Noah also has a longer soil moisture memory than OSU. At first glance this suggests that the soil moisture memory might play a part in the higher skill with Noah in that region. However, in MAM Noah still has a longer memory, while OSU has the higher skill. In this region Noah has longer soil moisture memory regardless of skill. In the south-central United States, the Sahel, and central Africa (and northern Australia, not shown) OSU generally has longer soil moisture memory, regardless of skill. In the Sahel the other

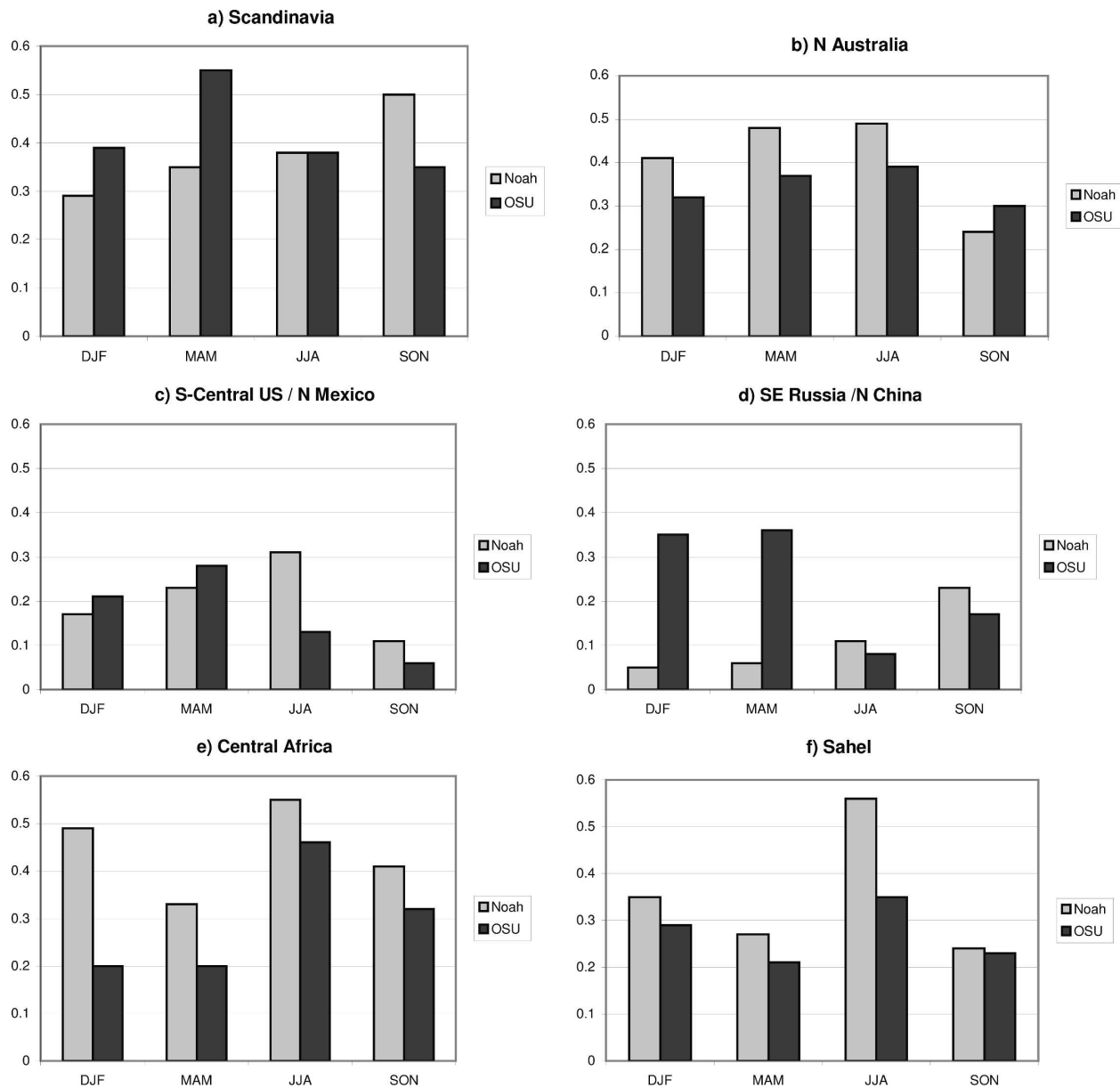


FIG. 11. Correlations between modeled—Noah and OSU—2-m seasonal mean temperatures and CRU observations averaged over the indicated regions for all four seasons: (a) Scandinavia, (b) northern Australia, (c) the south-central United States, (d) southeastern Russia and northern China, (e) central Africa, and (f) the Sahel.

three seasons produce soil moisture memory that is similar in the two ensembles. In northern China the soil moisture memory is also very similar between the two ensembles, both having high values (not shown). These results suggest that soil moisture memory does not usually have a role in the difference in skill between the two ensembles; rather it tends to be a function of location.

Clearly, this is not an exhaustive study and there could be areas or times that were not considered where soil moisture memory plays a significant role in skill.

However, those areas seem to be the exception, and most differences in skill between the two LSMs cannot be attributed to soil moisture memory alone. Further study into specific areas of improved skill is needed to determine the probable sources of the skill.

9. The Sahel

In previous sections it was shown that Noah improves upon OSU in the Sahelian precipitation climatology (Fig. 6), precipitation variability (Fig. 9), as well as

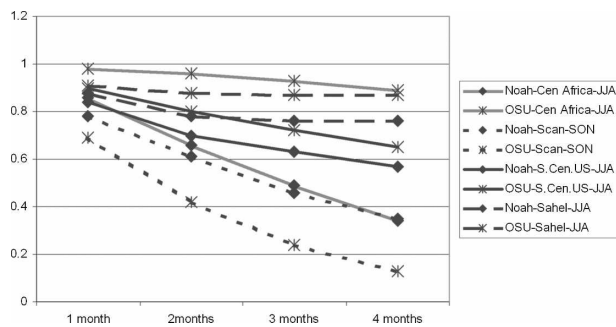


FIG. 12. Soil moisture auto time-lag correlations out to 4 months for Noah and OSU for the locations and seasons indicated.

near-surface temperature skill (Fig. 11). The precipitation improvements were related to the location of the maximum rainfall and variability band in Africa, which was too far south in OSU. The southward-shifted ITCZ resulted in too little rainfall and too little rainfall variability in OSU.

As we have already seen, there is an increase in 2-m temperature skill (temporal anomaly correlation of seasonal means with CRU data) on the order of 0.2 in JJA with Noah. In addition we find that there is a significant increase in precipitation skill in the Sahel in JJA, on the order of 0.1 in JJA. At points along the west coast of the Sahel, the increases in temporal precipitation anomaly correlation are as much as 0.3, and improvements are slightly larger when looking at July–September (JAS) instead of JJA. It should be noted that the ECPC SFM with the OSU LSM performed well in the Sahel in terms of precipitation and temperature skill compared with similar GCMs, but the Noah LSM has further enhanced its performance. To put the results in perspective, we consider the temporal correlation of the spatial average for precipitation in the Sahel. The average skill of six other state-of-the-art GCMs is 0.58, while OSU has a skill of 0.66 and Noah has a skill of 0.77 (M. Tippett 2006, personal communication).

A major part of the skill of the precipitation simulation in Noah is found to come from the drying trend, which occurs during the 1950s–80s as pointed out by Tippett (2006). Figure 13 shows the precipitation anomaly over the Sahel for Noah, OSU, and observations from CRU data, all smoothed with a 5-yr running mean. The anomalies for each are taken with respect to their own climatologies. The drying trend with Noah from 1950 to 1985 is quite similar to observations. However, almost no drying trend can be seen with OSU. This suggests that a major part of the increase in precipitation skill is due to the ability of Noah to capture the long-term trend.

Finally, we will consider the difference between the

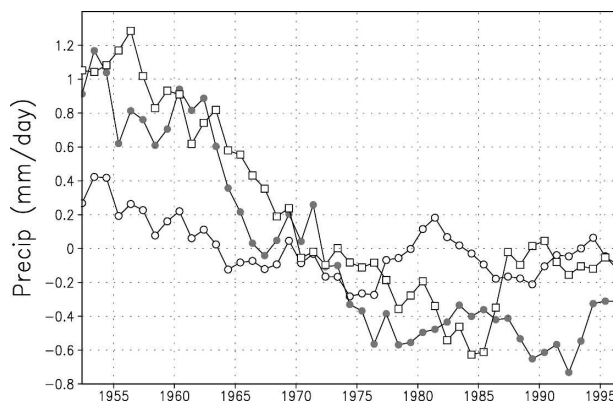


FIG. 13. Precipitation anomalies for the Sahel with a 5-yr running mean: CRU observed (open squares) Noah (filled circles), and OSU (open circles) (in mm day^{-1}).

two ensembles for the African easterly jet (AEJ) in western Africa. Figure 14 shows the vertical profile of the zonal wind from the equator to 30°N at 0° longitude. With Noah the AEJ can be seen at 600 hPa and 13°N , but it is not well defined and is too far south with OSU, centered at about 5°N . The improved AEJ is likely due in part to the improved soil moisture in Noah (Fig. 7), which could then improve the meridional temperature gradient and vertical wind shear. Cook (1999) proposed a soil moisture feedback mechanism as part of the formation of the AEJ, where more accurate soil moisture was necessary for the AEJ.

These results suggest that, in the Sahel, the improved overall climatology with Noah is responsible in part for the increase in skill. The improvements with Noah, which is the more physically realistic LSM, also suggest that accurate land surface processes are essential for high-quality simulations of the Sahel, in order to reproduce the correct response to SST forcing. Thiaw and Mo (2005), Druyan et al. (2004), Koster et al. (2004), and others have also shown a significant relationship between the land surface processes and precipitation prediction in the Sahel.

10. Attribution to changes in the LSMs

The purpose of this section is to address the relationship between the changes in climatologies, variabilities, and skills presented in the previous sections to specific changes in the LSMs. Generally speaking, however, this is very difficult. The differences between the LSMs result in nonlinear interactions with an atmospheric circulation as well as with other physical processes, making it difficult to detect the single cause of the differences in climatology. The change in large-scale circulation mentioned in section 5, and the change in

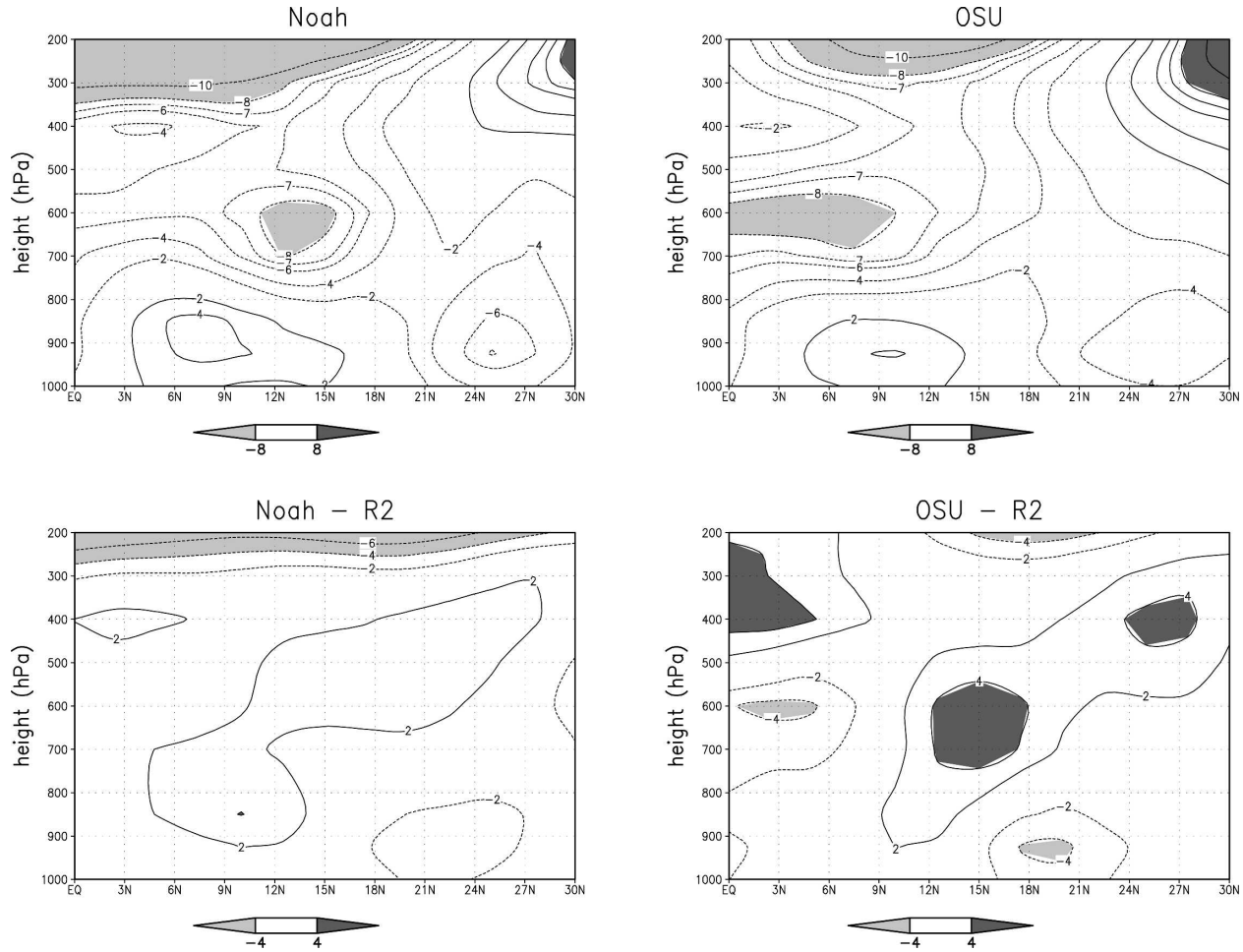


FIG. 14. Vertical profile of zonal wind at 0° longitude for JAS. (top) Full field and (bottom) differences between Noah and OSU with R2: (left) Noah and (right) OSU (in m s^{-1}).

precipitation due to the interaction between the LSM and convection processes are two such examples.

We can, however, make some direct assessments of the expected effects of the changes in the LSMs. We will look at three distinct differences between OSU and Noah: 1) the change in root zone, which was fixed in OSU but varies in Noah; 2) the change in the formulation of direct evaporation from bare soil, which is more sensitive in Noah due to the second-order dependency on soil moisture; and 3) the change in albedo, particularly the albedo of snow, which is fixed in OSU but varies with time and location in Noah.

By allowing the varying root zone depth (which is only possible with more levels), it is expected that areas with a shallower root zone will have overall wetter soil, since the atmosphere–soil interaction is limited in depth. However, we are not able to find any direct connection between root zone depth and soil moisture in the Noah simulation. We found those areas with

shorter root zone have more precipitation with the Noah LSM, masking the relation, and accordingly, it was not possible in this study to determine if the wetter soil is due to the reduced root zone depth.

With the changes to bare soil evaporation in the Noah LSM, we expect a stronger relationship between soil moisture and evaporation. The computation of the correlation between latent heat and soil moisture in nonsnowy areas in JJA was found to be 0.56 for OSU, and 0.69 for Noah, suggesting that the change in the direct evaporation formulation is actually detected in the simulation.

The Noah LSM utilizes variable maximum albedo (which is based on data in the Noah LSM), while it is a fixed value in OSU. We found that in Mongolia in MAM there is a large increase in albedo and a decrease in near-surface temperature in the Noah simulation compared to OSU, which can probably be attributed to the change in snow albedo. With the addition of patchy

snow to the Noah LSM, it is expected that the albedo will decrease and the surface temperature increase in those areas, but those differences are hard to see on a monthly mean time scale.

To find a relationship between the changes in the LSMs and the changes in variability or skill is more difficult. However, we believe that the improvement we found in Noah, particularly over Sahel, is due to the improvement of climatology over the area, which is likely the result of the change in the formulation of direct evaporation and root zone depth. However, an exact connection can only be detected by performing sensitivity studies.

11. Conclusions

Two sets of 10-member 53-yr AMIP integrations have been performed with the ECPC SFM. One set uses the state-of-the-art Noah land surface model, while the other uses the slightly older OSU land surface model.

The climatologies, variabilities, and anomaly correlations were compared between the two ensembles. For the temperature climatology, it was found that Noah produced a large warm bias in the northern latitudes, while OSU was somewhat closer to Reanalysis-2. The Noah precipitation climatology had more rainfall over land, and less over oceans than OSU. The magnitude of the precipitation bias was similar between the two ensembles. For the globally averaged variability, neither of the models produced the variability found in observations. Looking at the temporal anomaly correlations with CRU observations, Noah generally resulted in higher skill than OSU. Noah was significantly more skillful in three out of four seasons for 2-m temperature and was significantly more skillful in one season for precipitation (in the other three seasons there was not a significant difference in precipitation skill). This result was somewhat unexpected since the systematic error of Noah was generally larger than that of OSU. This indicates that the interaction between the time mean field and the model skill is not very strong, at least if we look at the skill globally, which is fairly well known.

It was also found that there was not a strong relationship between soil moisture memory and skill, indicating that the land surface model is important in passing the SST forcing correctly to the atmosphere through soil moisture memory, but soil moisture memory alone does not increase the prediction skill.

We also looked at the relationship between some of the changes in climatology, variability, and skill to changes in the LSM physics. The changes in root zone depth, the formulation of direct evaporation, and snow albedo resulted in limited information on attribution.

Additional sensitivity experiments are needed to study the physical processes that lead to the improvement of skill in Noah.

Looking regionally, it was found that central Africa (the Congo River basin) had large improvements with Noah. Noah removed a warm-dry bias that was present in OSU in that region and created higher skill.

One of the most significant improvements in the ECPC SFM with Noah is in the Sahel region of Africa. The temperature climatology, precipitation climatology, and precipitation variability were all more realistic with Noah than OSU. Noah also increased the skill, both in temperature and precipitation, especially in the western Sahel. Although, in general there is not a strong relationship between climatology and skill, it is likely that this region is an exception, where improved climatology and variability lead to improved skill. Much of the improved skill came from the ability of Noah to reproduce the drying trend in the Sahel from the 1950s to the 1980s. In addition, there was improvement in the location of the ITCZ, which likely led to improved temperature gradients, and improved large-scale circulation, particularly the representation of the AEJ. These improvements are especially noteworthy since the OSU version of the ECPC SFM already performed quite well in the Sahel.

It is clear from our results that a given global model configuration can perform well for some regions (i.e., the Sahel and central Africa) but not for others (i.e., central Canada). This is an added challenge over regional models, which can be optimized for locations of interest, but is also valuable information for regional modelers choosing an LSM for a specific region.

In addition, the improvements in the Sahel point to the importance of a realistic land surface model in such semiarid regions, and also to the importance of correctly simulating the climatology. Apparently, over some regions in tropical semiarid areas, the interaction between mean fields and skill are strong, and a correct simulation of the climatology is essential. This is in contrast to the extratropics, where the interaction between systematic error and skill is not so strong. It is also worthy to note that the combination of high skill and accurate climatology and variability make the ECPC SFM an excellent tool for further study of the Sahel.

Acknowledgments. The authors gratefully acknowledge the help of Michael Tippett and three anonymous reviewers. This study was supported by NOAA NA17RJ1231. The views expressed herein are those of the authors and do not necessarily reflect the views of NOAA. Several figures were created with GrADS software.

REFERENCES

- Alpert, J. C., M. Kanamitsu, P. M. Caplan, J. G. Sela, G. H. White, and E. Kalnay, 1988: Mountain induced gravity wave drag parameterization in the NMC medium-range model. Preprints, *Eighth Conf. on Numerical Weather Prediction*, Baltimore, MD, Amer. Meteor. Soc., 726–733.
- Basist, A. N., and M. Chelliah, 1997: Comparison of tropospheric temperatures derived from the NCEP/NCAR Reanalysis, NCEP operational analysis, and the microwave sounding unit. *Bull. Amer. Meteor. Soc.*, **78**, 1431–1447.
- Betts, A. K., F. Chen, K. E. Mitchell, and Z. I. Janic, 1997: Assessment of the land surface and boundary layer models in two operational versions of the NCEP Eta Model using FIFE data. *Mon. Wea. Rev.*, **125**, 2896–2916.
- Bonan, G. B., K. W. Oleson, M. Vertenstein, S. Levis, X. Zeng, Y. Dai, R. E. Dickinson, and Z. L. Yang, 2002: The land surface climatology of the community land model coupled to the NCAR community climate model. *J. Climate*, **15**, 3123–3149.
- Chen, F., and J. Dudhia, 2001: Coupling an advanced land surface–hydrology model with the Penn State–NCAR MM5 modeling system. Part I: Model implementation and sensitivity. *Mon. Wea. Rev.*, **129**, 569–585.
- , and Coauthors, 1996: Modeling of land surface evaporation by four schemes and comparison with FIFE observations. *J. Geophys. Res.*, **101**, 7251–7268.
- Chou, M.-D., and M. J. Suarez, 1994: An efficient thermal infrared radiation parameterization for use in general circulation models. Technical Report Series on Global Modeling and Data Assimilation, NASA Tech. Memo. TM-1994-104606, Vol. 3, 85 pp.
- , and K.-T. Lee, 1996: Parameterizations for the absorption of solar radiation by water vapor and ozone. *J. Atmos. Sci.*, **53**, 1203–1208.
- Cook, K. H., 1999: Generation of the African easterly jet and its role in determining West African precipitation. *J. Climate*, **12**, 1165–1184.
- DeHaan, L. L., and M. Kanamitsu, 2007: Increase in near-surface temperature simulation skill due to predictive soil moisture in a numerical seasonal simulation under observed SST forcing. *J. Hydrometeorol.*, in press.
- Delage, Y., and D. Verseghy, 1995: Testing the effects of a new land surface scheme and of initial soil moisture conditions in the Canadian global forecast model. *Mon. Wea. Rev.*, **123**, 3305–3317.
- Dirmeyer, P. A., 2005: The land surface contribution to the potential predictability of boreal summer season climate. *J. Hydrometeorol.*, **6**, 618–632.
- , X. Gao, M. Zhao, Z. Guo, T. Oki, and N. Hanasaki, 2006: GSWP-2: Multimodel analysis and implications for our perception of the land surface. *Bull. Amer. Meteor. Soc.*, **87**, 1381–1397.
- Druryan, L. M., M. Fulakeza, and P. Lonergan, 2004: Land surface influences on the West African summer monsoon: Implications for synoptic disturbances. *Meteor. Atmos. Phys.*, **86**, 261–273.
- Ek, M., and L. Mahrt, 1991: A formulation for boundary-layer cloud cover. *Ann. Geophys.*, **9**, 716–724.
- , K. E. Mitchell, Y. Lin, E. Rogers, P. Grunmann, V. Koren, G. Gayno, and J. D. Tarpley, 2003: Implementation of Noah land surface model advances in the National Centers for Environmental Prediction operational mesoscale Eta Model. *J. Geophys. Res.*, **108**, 8851, doi:10.1029/2002JD003296.
- Garratt, J. R., 1993: Sensitivity of climate simulations to land-surface and atmospheric boundary-layer treatments: A review. *J. Climate*, **6**, 419–448.
- Hou, Y., S. Moorthi, and K. Campana, 2002: Parameterization of solar radiation transfer in the NCEP models. NCEP Office Note 441, 34 pp. [Available online at www.emc.ncep.noaa.gov/officenotes/FullTOC.html#2000.]
- Kalnay, E., and Coauthors, 1996: The NCEP/NCAR 40-Year Reanalysis Project. *Bull. Amer. Meteor. Soc.*, **77**, 437–471.
- Kanamitsu, M., and K. C. Mo, 2003: Dynamical effect of land surface processes on summer precipitation over the southwestern United States. *J. Climate*, **16**, 496–509.
- , and Coauthors, 2002a: NCEP dynamical seasonal forecast system 2000. *Bull. Amer. Meteor. Soc.*, **83**, 1019–1037.
- , W. Ebisuzaki, J. Woolen, S.-K. Yang, J. J. Hnilo, M. Fiorino, and J. Potter, 2002b: NCEP–DOE AMIP-II Reanalysis (R2). *Bull. Amer. Meteor. Soc.*, **83**, 1631–1643.
- Kim, Y.-J., and A. Arakawa, 1995: Improvement of orographic gravity wave parameterization using a mesoscale gravity wave model. *J. Atmos. Sci.*, **52**, 1875–1902.
- Koren, V., J. Schaake, K. Mitchell, Q.-Y. Duan, F. Chen, and J. M. Baker, 1999: A parameterization of snowpack and frozen ground intended for NCEP weather and climate models. *J. Geophys. Res.*, **104**, 19 569–19 585.
- Koster, R. D., and M. J. Suarez, 1992: Modeling the land surface boundary in climate models as a composite of independent vegetation stands. *J. Geophys. Res.*, **97**, 2697–2715.
- , P. A. Dirmeyer, A. N. Hahmann, R. Ijpeelaar, L. Tyahla, P. Cox, and M. J. Saurez, 2002: Comparing the degree of land–atmosphere interaction in four atmospheric general circulation models. *J. Hydrometeorol.*, **3**, 363–375.
- , and Coauthors, 2004: Regions of strong coupling between soil moisture and precipitation. *Science*, **305**, 1138–1140.
- Liang, X., D. P. Lettenmaier, E. F. Wood, and S. J. Burges, 1994: A simple hydrologically based model of land surface water and energy fluxes for general circulation models. *J. Geophys. Res.*, **99**, 14 415–14 428.
- Lu, C.-H., M. Kanamitsu, J. O. Roads, W. Ebisuzaki, K. Mitchell, and D. Lohmann, 2005: Evaluation of soil moisture in the NCEP–NCAR and NCEP–DOE global reanalyses. *J. Hydrometeorol.*, **6**, 391–408.
- Mahfouf, J. F., and J. Noilhan, 1991: Comparative study of various formulations of evaporations from bare soil using in situ data. *J. Appl. Meteor.*, **30**, 1345–1365.
- Mahrt, L., and M. Ek, 1984: The influence of atmospheric stability on potential evaporation. *J. Climate Appl. Meteor.*, **23**, 222–234.
- , and H. L. Pan, 1984: A two layer model for soil hydrology. *Bound.-Layer Meteorol.*, **29**, 1–20.
- Maynard, K., and J. Polcher, 2003: Impact of land-surface processes on the interannual variability of tropical climate in the LMD GCM. *Climate Dyn.*, **20**, 613–633.
- Mesinger, F., and Coauthors, 2006: North American Regional Reanalysis. *Bull. Amer. Meteor. Soc.*, **87**, 343–360.
- Mitchell, K. E., and Coauthors, 2004a: The multi-institution North American Land Data Assimilation System (NLDAS): Utilizing multiple GCIP products and partners in a continental distributed hydrological modeling system. *J. Geophys. Res.*, **109**, D07S90, doi:10.1029/2003JD003823.
- , and Coauthors, 2004b: NCEP completes 25-year North American Reanalysis: Precipitation assimilation and land surface are two hallmarks. *GEWEX News*, Vol. 14, International GEWEX Project Office, Silver Spring, MD, 9–12.

- Mlawer, E. J., S. J. Taubman, P. D. Brown, M. J. Iacono, and S. A. Clough, 1997: Radiative transfer for inhomogeneous atmospheres: RRTM, a validated correlated- k model for the longwave. *J. Geophys. Res.*, **102**, 16 663–16 682.
- Moorthi, S., and M. J. Suarez, 1992: Relaxed Arakawa–Schubert: A parameterization of moist convection for general circulation models. *Mon. Wea. Rev.*, **120**, 978–1002.
- Pan, H.-L., and L. Mahrt, 1987: Interaction between soil hydrology and boundary layer developments. *Bound.-Layer Meteor.*, **38**, 185–202.
- Pan, M., and Coauthors, 2003: Snow process modeling in the North American Land Data Assimilation System (NLDAS): 2. Evaluation of model simulated snow water equivalent. *J. Geophys. Res.*, **108**, 8850, doi:10.1029/2003JD003994.
- Peters-Lidard, C. D., M. S. Zion, and E. F. Wood, 1997: A soil-vegetation-atmosphere transfer scheme for modeling spatially variable water and energy balance processes. *J. Geophys. Res.*, **102**, 4303–4324.
- Roads, J. O., S.-C. Chen, M. Kanamitsu, and H. Juang, 1999: Surface water characteristics in the NCEP global spectral model and reanalysis. *J. Geophys. Res.*, **104**, 19 307–19 327.
- , and Coauthors, 2003: The International Research Institute/Applied Research Centers (IRI/ARCs) regional model intercomparison over South America. *J. Geophys. Res.*, **108**, 4425, doi:10.1029/2002JD003201.
- Robock, A., and Coauthors, 2003: Evaluation of the North American Land Data Assimilation System over the southern Great Plains during the warm season. *J. Geophys. Res.*, **108**, 8846, doi:10.1029/2002JD003245.
- Rodell, M., and Coauthors, 2004: The Global Land Data Assimilation System. *Bull. Amer. Meteor. Soc.*, **85**, 381–394.
- Saha, S., and Coauthors, 2006: The NCEP Climate Forecast System. *J. Climate*, **19**, 3483–3517.
- Schaake, J. C., and Coauthors, 2004: An intercomparison of soil moisture fields in the North American Land Data Assimilation System (NLDAS). *J. Geophys. Res.*, **109**, D01S90, doi:10.1029/2002JD003309.
- Sheffield, J., and Coauthors, 2003: Snow process modeling in the North American Land Data Assimilation System (NLDAS): 1. Evaluation of model-simulated snow cover extent. *J. Geophys. Res.*, **108**, 8849, doi:10.1029/2002JD003274.
- Slingo, J. M., 1987: The development and verification of a cloud prediction scheme for the ECMWF model. *Quart. J. Roy. Meteor. Soc.*, **113**, 899–927.
- Thiaw, W. M., and K. C. Mo, 2005: Impact of sea surface temperature and soil moisture on seasonal rainfall prediction over the Sahel. *J. Climate*, **18**, 5330–5343.
- Tiedtke, M., 1983: The sensitivity of the time-mean large-scale flow to cumulus convection in the ECMWF model. *Proc. ECMWF Workshop on Convection in Large-Scale Models*, Reading, United Kingdom, European Centre for Medium-Range Weather Forecasts, 297–316.
- Tippett, M. K., 2006: Filtering of GCM simulated Sahel precipitation. *Geophys. Res. Lett.*, **33**, L01804, doi:10.1029/2005GL024923.
- Winton, M., 2000: A reformulated three-layer sea ice model. *J. Atmos. Oceanic Technol.*, **17**, 525–531.
- Yulaeva, E., M. Kanamitsu, and J. Roads, 2007: The ECPC Coupled Prediction Model. *Mon. Wea. Rev.*, in press.
- Zhao, Q., and F. H. Carr, 1997: A prognostic cloud scheme for operational NWP models. *Mon. Wea. Rev.*, **125**, 1931–1953.